AIRBORNE TWO-MICRON DOUBLE-PULSE IPDA LIDAR VALIDATION FOR CARBON DIOXIDE MEASUREMENTS OVER LAND

Tamer F. Refaat[1]*, Upendra N. Singh[1], Jirong Yu[1], Mulugeta Petros[1], Ruben Remus[1] & Syed Ismail[2]

[1]NASA Langley Research Center, Hampton, VA 23681, USA,
**Email: tamer.f.refaat@nasa.gov*
[2]Analytical Services and Materials, Inc., Hampton, VA 23666, USA

ABSTRACT

An airborne double-pulse 2-μm Integrated Path Differential Absorption (IPDA) lidar has been developed at NASA LaRC for measuring atmospheric CO_2. IPDA was validated using NASA B-200 aircraft over land and ocean under different conditions. IPDA evaluation for land vegetation returns, during full day background conditions, are presented. IPDA CO_2 measurements compare well with model results driven from on-board *in-situ* sensor data. These results also indicate that CO_2 measurement bias is consistent with that from ocean surface returns.

1 INTRODUCTION

Atmospheric carbon dioxide (CO_2) plays a key role in Earth's environment and climate and it influences processes in the atmosphere, biosphere, and hydrosphere. Large uncertainties in quantifying CO_2 fluxes arise due to data quality and insufficient spatial and temporal coverage of the gas distributions. Active optical remote sensing has been recommended to improve the understanding of CO_2 fluxes including sources and sinks. For more than 20 years, NASA Langley Research Center (LaRC) has been involved in maturing 2-μm technologies, including pulsed laser transmitters, for lidar systems that are focused on meeting the science objectives for CO_2 measurements. Recently, an airborne CO_2 double-pulse 2-μm integrated path differential absorption (IPDA) lidar was developed at LaRC [1-3].

Airborne field experiments were conducted using NASA B-200 aircraft to test and evaluate the CO_2 measurement capabilities of the 2-μm IPDA. The IPDA was tuned to the CO_2 R30 strong absorption line at 2050.9670 nm. This line is optimum for lower tropospheric weighted column CO_2 sensing. Flights were conducted over land and ocean under different conditions. Initial IPDA validation focused on low reflectivity oceanic surface returns during full day background conditions [3]. On April 5, 2014 IPDA CO_2 measurements were compared to airborne flask air-sampling CO_2 measurements conducted by NOAA over the Atlantic Ocean. IPDA performance modeling was conducted to evaluate measurement sensitivity and bias errors. IPDA signals compare well with predicted model results including altitude dependence. Off-off-line testing was conducted to evaluate the IPDA systematic and random errors. Results over the ocean showed altitude-independent differential optical depth offset of 0.0769. Measured CO_2 differential optical depth random error of 0.0918 compared well with the predicted value of 0.0761. IPDA CO_2 column measurement compared well with model-driven, concurrent different altitude air-sampling from NOAA. CO_2 differential optical depth of 1.0054 ±0.0103 was retrieved from 6-km altitude, 4-GHz offset on-line operation and 10 s average. IPDA ranging resulted in less than 3 m uncertainty [3].

In this paper a separate B-200 airborne validation experiment for the 2-μm IPDA lidar will be presented. On April 10, 2014, the IPDA was evaluated over East Virginia vegetation targets, from different altitudes. On board aircraft sensors, *in-situ* sensor (LiCor) and balloon sonde were used to obtain CO_2 and meteorological profiles. These profiles were applied to model and compare with CO_2 column IPDA measurements over land. Careful analysis allows reduction or elimination of range biases with the pulsed IPDA.

2 METEOROLOGY

Meteorological data are required for IPDA lidar modeling and retrievals. These data are acquired from other instruments and can limit the accuracy of IPDA measurements. In this analysis, temperature and pressure profiles were obtained from balloon sonde. Dry-air H_2O and CO_2 mixing ratios, x_{wv} and x_{cd}, were obtained from aircraft and *in-situ* sensors. US standard atmospheric (USSA) model was included as a reference. Figure 1 shows the NASA-B200 GPS altitude, R_A, and line-of-sight distance, R_L, obtained using the roll and pitch angles. Ground elevation, R_G, was obtained from Google Maps Application Programming Interface web-service [4].

Figure 2 shows altitude profiles of x_{wv} obtained from sonde and aircraft and *in-situ* sensors compared with USSA model. The figure also shows x_{cd} profiles obtained from *in-situ* compared to USSA with updated surface level of 411 ppm. A 2 km boundary layer (BL) height could be estimated from x_{wv} profiles. This is indicated from fixed amount within BL followed by sharp drop in lower troposphere. Near-surface high x_{wv} deviation between sonde and *in-situ* profiles is observed in BL with closer match at higher altitudes. CO_2 profile shows lower near-surface amounts due to photosynthesis followed by gradual increase toward BL top. Sharp decline in lower troposphere indicates CO_2 trapping. Data clusters in both x_{cd} and x_{wv} profiles are due to fixed altitudes flight track, as listed in Table 1. Statistical analysis conducted for these clusters to obtain mean and standard deviation. Linear interpolation was used to join the means and linear extrapolation to extend profiles down to surface and up to 4.5 km altitude.

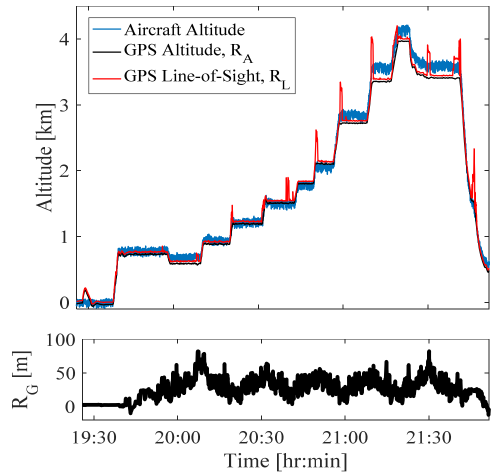

Figure 1 April 10, 2014 NASA B-200 flight altitude, obtained from aircraft sensors and GPS, the derived line-of-sight distance (top) and the corresponding ground elevation, R_G (bottom).

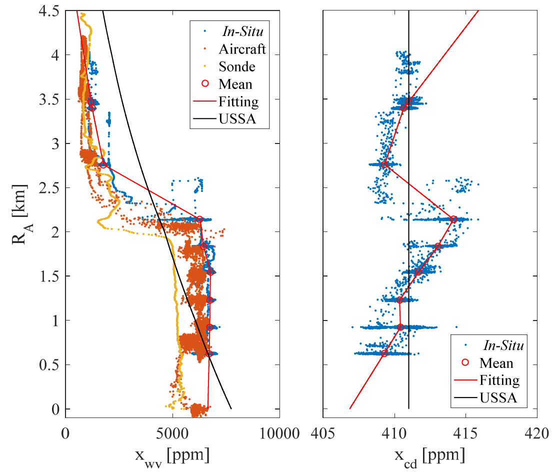

Figure 2 Comparison between x_{wv} (left) and x_{cd} (right) profiles obtained from different sensors and fittings.

3 IPDA MODELING

The 2-µm IPDA measured double-path optical depth mainly results from CO_2 and H_2O absorption and aerosol optical depths. The CO_2 double-path differential optical depth, $\Delta\tau_{cd}$, can be modeled as

$$\Delta\tau_{cd} = 2 \cdot \int_{R_A}^{R_G} \Delta\sigma_{cd} \cdot N_{cd} \cdot dr \quad (1)$$

for a nadir airborne IPDA at an altitude R_A operating over ground elevation R_G; $\Delta\sigma_{cd}$ is the CO_2 differential absorption cross section obtained at on- and off-line wavelengths, λ_{on} and λ_{off}, respectively; N_{cd} is the CO_2 number density (in m^{-3}); and r is the range. In this equation, aerosols optical depth cancel due to the small on- and off-line wavelength separation in $\Delta\sigma_{cd}$ measurements.

H_2O interference is not included due to relatively lower differential optical depth. For example, modeling indicated the highest H_2O interference error on CO_2 measurement is 0.09% at 624.2 m altitude the nearest to the surface.

Figure 3 shows the predicted CO_2 differential optical depth using both *in-situ* and USSA model for this flight. On-line wavelengths were set at 3 and 4 GHz offsets from line center. Agreement between *in-situ* and USSA model in $\Delta\tau_{cd}$ estimates is attributed to R30 line properties, characterized by low temperature dependence and low H_2O interference. The figure also shows the IPDA measurements and modeling over ocean surface for comparison with land vegetation targets [3].

4 IPDA MEASUREMENTS

During this IPDA validation, the instrument was operated almost continuously with on-line set to 3 GHz. Similar to the ocean validation, analysis is focused on high-signal detection channel. Trans-impedance amplifier (TIA) gain was set to 10^3 V/A for lowest altitudes (up to 1.3 km) and 10^4 V/A for higher altitudes, with digitizer full-scale range of 1 and 2 V, respectively. This was done to avoid saturation and increase signal-to-noise ratio (SNR). Figure 4 shows on- and off-line sample return signals from different altitudes.

4.1 Ranging

IPDA column length, R_C, was obtained by converting the time delay between the near-field residual scattering and return pulse peaks into distance using the speed of light. Table 1 lists ranging results corresponding to the averaged data cluster timings. Figure 5 compares R_C to R_L at three altitudes. Less than 3 m IPDA range accuracy was demonstrated over ocean and calibrated targets [2-3]. Larger error in IPDA column length measurement ($\varepsilon_R = \delta(R_C–R_L)$) was observed over land that is a characteristic of range variability due to vegetation (trees).

4.2 CO_2 differential optical depth

IPDA measured $\Delta\tau_{cd}$ is obtained by ratioing the return power, P, return pulse width, t, and transmitted laser energy, E, for the on- and off-line wavelengths, according to

$$\Delta\tau_{cd} = \ln\left[\frac{P_{off}\cdot t_{off}}{E_{off}} \bigg/ \frac{P_{on}\cdot t_{on}}{E_{on}}\right] \qquad (2)$$

Table 2 lists statistical results of the IPDA $\Delta\tau_{cd}$ measurement mean, $\Delta\tau_{cd,g}$, as compared to simulation prediction, $\Delta\tau_{cd,c}$. A comparison of these results that are similar to those from ocean target are included in Figure 3 [3]. The observed offset or bias at each altitude, $\Delta(\Delta\tau_{cd})$, is the difference between the *in-situ* driven model and Gaussian mean (i.e., $\Delta(\Delta\tau_{cd}) = \Delta\tau_{cd,g} - \Delta\tau_{cd,c}$). Similar to ocean surface observations, IPDA bias trends higher at higher altitudes and via versa. These biases are consistent in spite of IPDA operation at 3 and 4 GHz over ocean and only at 3 GHz over land.

Table 1 Comparison between flight altitude, ground elevation, line-of-sight, IPDA column measurement and column measurement uncertainty (in m).

R_A	R_G	R_L	R_C	ε_R
3394.1	30.2	3363.9	3366.0	6.8
2759.9	30.4	2729.5	2729.1	7.0
2140.3	34.1	2106.2	2111.3	7.5
1838.6	34.0	1804.6	1807.8	7.4
1544.5	27.2	1517.3	1527.6	8.0
1228.7	29.7	1199.0	1201.1	6.6
920.8	31.4	889.4	894.9	8.2
624.2	43.9	580.3	585.5	7.6

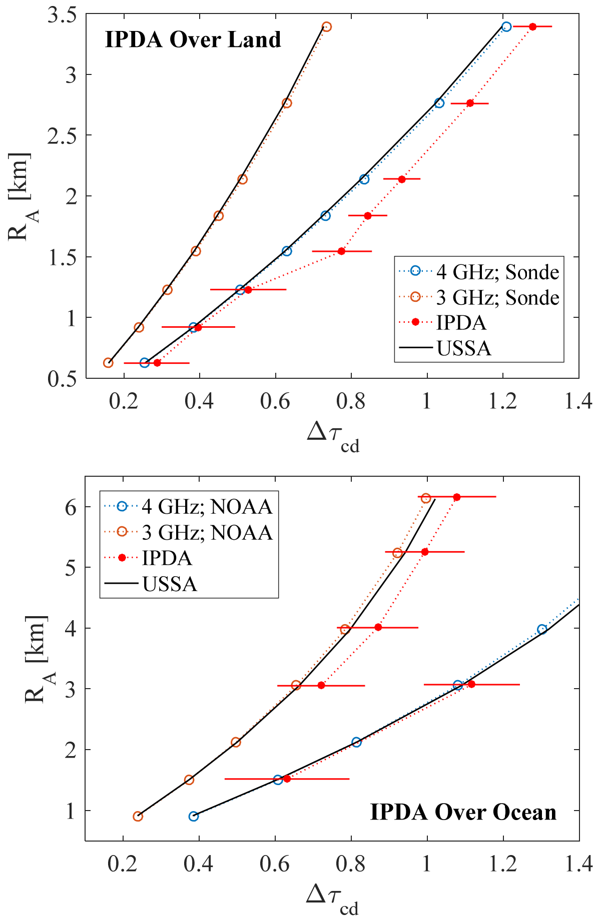

Figure 3 Comparison between IPDA CO_2 differential optical depth early afternoon measurements and simulations over land vegetation (top) and ocean (bottom). Land and ocean simulations were obtained from in-situ and NOAA air-sampling, respectively [3].

Characterization of the higher altitude bias through off-off line testing over ocean revealed consistent results [3]. Although these biases were originally attributed to the TIA, different TIA gain settings were used in this flight as compared to the ocean flight. This indicates that the digitizer is more likely the reason for such offsets. At low altitudes digitizer input was set to lower full-scale range than higher altitudes to accommodate TIA gain settings. Digitizer different input ranges resulted in different biases. This is confirmed for both IPDA validations over ocean and land.

5 CONCLUSIONS

Airborne double-pulse 2-µm IPDA lidar capability for CO_2 remote sensing was demonstrated over land and ocean. As an active remote sensor, this IPDA is capable of enhancing spatial and temporal resolution of CO_2 measurement over different target conditions during day and night. IPDA operation at the strong CO_2 R30 line at 2050.9670 nm allows optimum lower tropospheric weighted column measurements with low temperature dependence and H_2O interference errors. IPDA modeling was conducted for nadir operation targeting land vegetation at variable elevations using USSA model and meteorological data collected by on-board LiCor *in-situ* sensor and balloon sonde. CO_2 differential optical depth measurement biases are consistent for different flights, over land and ocean, and correlates with digitizer settings, which can be characterized by off-off line IPDA testing.

ACKNOWLEDGEMENTS

This work was funded and supported by NASA Earth Science Technology Office.

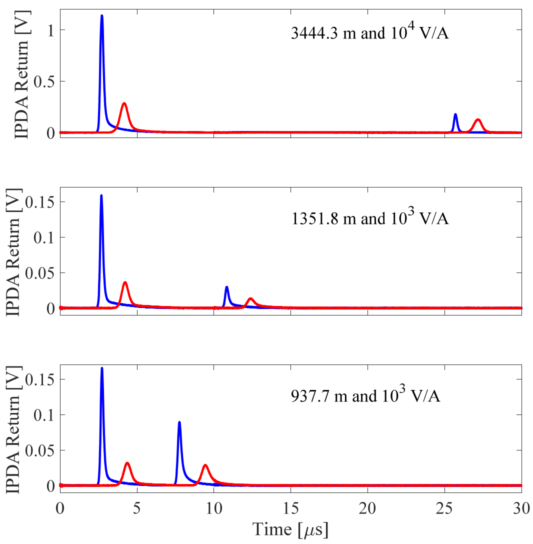

Figure 4 100-shot (10 s) averaged on-line (blue) and off-line (red) return signals from different altitudes.

Table 2 Statistical comparison of simulated and measured 2-µm IPDA CO_2 double-path differential optical depth.

R_A	$\Delta\tau_{cd,c}$	$\Delta\tau_{cd,g}$	$\delta(\Delta\tau_{cd,g})$	$\Delta(\Delta\tau_{cd})$
3394.1	1.2088	1.2778	0.0515	0.0690
2759.9	1.0325	1.1122	0.0500	0.0797
2140.3	0.8355	0.9331	0.0489	0.0976
1838.6	0.7319	0.8433	0.0516	0.1114
1544.5	0.6288	0.7752	0.0789	0.1463
1228.7	0.5078	0.5280	0.1007	0.0202
920.8	0.3851	0.3963	0.0970	0.0112
624.2	0.2560	0.2862	0.0867	0.0302

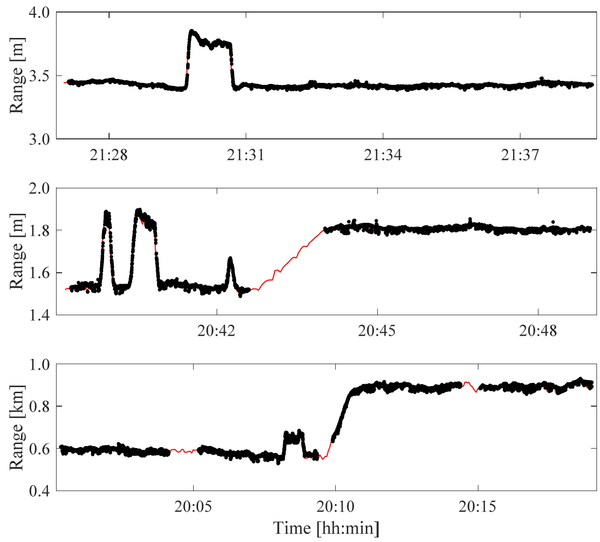

Figure 5 Comparison between IPDA lidar column length measurements (per-shot black dots) and line-of-sight (red profiles) at different altitudes.

References

[1] U. Singh, B. Walsh, J. Yu, M. Petros, M. Kavaya, T. Refaat, N. Barnes, 2015: Twenty years of Tm:Ho:YLF and LuLiF laser development for global wind and carbon dioxide active remote sensing, *Opt. Mater. Exp.* **5**, 827-837.

[2] T. Refaat, U. Singh, M. Petros, R. Remus, J. Yu, 2015: Self-calibration and laser energy monitor validations for a double-pulsed 2-µm CO_2 integrated path differential absorption lidar application, *Appl. Opt.* **54**, 7240-7251.

[3] T. Refaat, U. Singh, J. Yu, M. Petros, R. Remus, S. Ismail, 2015: Double-pulse 2-µm integrated path differential absorption lidar airborne validation for atmospheric carbon dioxide measurement, *Appl. Opt.* **55**, 4232-4246.

[4] *https://developers.google.com/maps/documentation/elevation*